PHYSICAL REVIEW A **71**, 011801(R) (2005)

Improvement of signal-to-noise ratio in a bistable optical system: Comparison between vibrational and stochastic resonance

V. N. Chizhevsky[1,2] and Giovanni Giacomelli[1,3]
[1]*Istituto Nazionale di Ottica Applicata, Largo E. Fermi 6, 50125 Firenze, Italy*
[2]*B. I. Stepanov Institute of Physics, NASB, 220072 Minsk, Belarus*
[3]*Istituto Nazionale di Fisica della Materia, Unità di Firenze, Firenze, Italy*
(Received 24 May 2004; published 6 January 2005)

We present an experimental and theoretical study of the effect of additive noise on the signal-to-noise ratio (SNR) in a bistable, vertical cavity laser. We show that, the regime of vibrational resonance leads to higher SNR's than the regime of stochastic resonance. A scaling law for the noise-induced degradation of SNR is obtained analytically and compared with experimental and numerical results, showing a good agreement.

DOI: 10.1103/PhysRevA.71.011801 PACS number(s): 42.60.Mi, 42.55.Px, 42.65.Sf, 05.40.Ca

In the last years, in the context of stochastic resonance (SR) [1], large efforts have been devoted to finding conditions for the improvement of the detection of weak noisy signals. This subject is a matter of great interest in different fields and is not a trivial problem. As a rule, the quality in the detection of periodic signals can be evaluated using the signal-to-noise ratio (SNR). A theoretical treatment using the concept of SR has revealed that a SNR gain [that is, the output $(\mathrm{SNR})_{out}$ is higher than the input $(\mathrm{SNR})_{in}$] can be achieved in level crossing detectors [2], nondynamical threshold systems with a static nonlinearity [3], in bistable dynamical systems for a periodic sequence of alternating rectangular pulses with a small duty cycle and near-threshold amplitudes [4,5], and in a Schmidt trigger with near-threshold rectangular pulses [6,7]. Evidence of the SNR gain was given in a Schmitt trigger [6] and in an analog simulation [4].

Recently, the phenomenon of vibrational resonance (VR) has been theoretically predicted by Landa and McClintock [8]. Experimental evidence of VR has been demonstrated in analog circuits [10–12] and in a bistable vertical cavity surface emitting laser (VCSEL) [13]. The phenomenon shows up in a bistable system as a resonancelike behavior in the response at the low-frequency (LF), depending on the amplitude or frequency of an additional high-frequency (HF), modulation. The mechanism underlying VR can be associated with a parametric amplification near the onset of bistability controlled by the high-frequency modulation. In this case SNR is determined by two processes, namely, the amplification of the LF periodic signal and enhancement of fluctuations near the bifurcation point. The interplay between these two processes near the critical point determines the resulting SNR. Since no additional noise is added to the system, one can expect that the output SNR can be improved with respect to the input.

Here we present a theoretical and experimental study of the effect of additive noise on SNR in a bistable optical system. We show that (i) the noise-induced degradation of SNR obeys a simple scaling law, (ii) SNR in VR for weak periodic signals is always higher than the one which could be obtained in the same conditions using conventional SR, and, (iii) the experimental and numerical evidence that the relationship $(\mathrm{SNR})_{out} \gg (\mathrm{SNR})_{in}$ can be achieved for rectangular periodic LF signals with weak subthreshold amplitudes in a broad range of the level of initial noise coming together with the signal.

First, we present some analytical results on the behavior of SNR due to VR depending on the initial noise level in a model of an overdamped bistable oscillator. For the sake of clarity, we recall some of the results presented in [12]. The system is being excited by the LF periodic signal $f(\Omega_L)$ with a frequency Ω_L and an amplitude A_L, and by a sinusoidal HF modulation with an amplitude A_H and a frequency Ω_H, such that $\Omega_H \gg \Omega_L$. In this case, the dynamics is described by the equation

$$\partial x/\partial t = -V'(x) + A_L f(t) + A_H \sin \Omega_H t, \tag{1}$$

where $V'(x)$ is the derivative with respect to x of a bistable potential function $V(x) = -\alpha x^2/2 + \beta x^4/4$, with local minima $x_m^{\pm} = \pm\sqrt{\alpha/\beta}$ and barrier height $V_0 = \alpha^2/4\beta$, where α and β are positive numbers. The dynamics is ruled by two time scales which are determined by LF and HF signals, respectively. Therefore, we look for the solution as follows [9]: $x(t) = y(t) + [A_H/(\Omega_H^2 + \eta)^{1/2}]\cos \Omega_H t$ where $y(t)$ denotes the slow part of the solution and η is a parameter. Substituting it into (1) and averaging over the period $T_H = 2\pi/\Omega_H$, we obtain the following equation, which governs a slow dynamics of the system:

$$dY/dt = \alpha(1 - \xi^2)Y - \beta Y^3 + A_L F(t), \tag{2}$$

where $Y = \langle y(t)\rangle_{T_H}$, $F(t) = \langle f(t)\rangle_{T_H}$, and where $\langle z(t)\rangle_{T_H} = 1/T_H \int_0^{T_H} z(T)dT$. We introduce here a normalized parameter $\xi = A_H/A_c$, where A_c is a switching threshold which depends on both the amplitude and the frequency $A_c = [(2\alpha/3\beta)(\Omega_H^2 + 2\alpha^2/9\beta)]^{1/2}$. In this case, the effective potential $V_{eff}(x)$ takes the form

$$V_{eff}(x, \xi) = -\alpha(1 - \xi^2)x^2/2 + \beta x^4/4. \tag{3}$$

The sign near the quadratic term determines the character of $V_{eff}(x, \xi)$. For $\xi = 1$ we have a bifurcation point where the transition from bistability to monostability occurs as ξ increases [12]. Obviously, after averaging, the parameters of

the potential such as the minima location $x_m^{\pm}$ and the barrier height V_ξ depend on ξ,

$$x_m^{\pm} = \pm\sqrt{\alpha(1-\xi^2)/\beta}, \quad V_\xi = \alpha^2(1-\xi^2)^2/4\beta. \tag{4}$$

Now, we can study the effect of noise on SNR for the LF signal $F(t)=\sin(\Omega_L t)$. In this case the equation reads

$$dY/dt = \alpha(1-\xi^2)Y - \beta Y^3 + A_L\sin(\Omega_L t) + \zeta(t), \tag{5}$$

where $\zeta(t)$ is a white, Gaussian noise with $\langle\zeta(t)\zeta(t')\rangle = 2D\delta(t-t')$ and mean $\langle\zeta(t)\rangle=0$. We explicitly assume here that the averaging does not change the character of noise when we add the noise term into the averaged equation. Equation (5) is the standard statement of the problem used for studying the phenomenon of SR. We can use therefore the analytical results obtained earlier, taking into account the dependence of the potential parameters on ξ. In particular, we consider here the well-known result for SNR in SR. In the limit $x_m A_L \ll D$, the SNR can be evaluated from the expression [see, for instance, Eq. (3.12) from [14]]

$$R = \pi(A_L x/D)^2 r_k, \tag{6}$$

where

$$r_k = \frac{\alpha(1-\xi^2)}{\sqrt{2}\pi}\exp\left(-\frac{\alpha^2(1-\xi^2)^2}{4\beta D}\right) \tag{7}$$

is the Kramers rate. Substituting x_m (4) and r_k (7) into (6), we obtain for SNR in VR (denoted as R_{VR})

$$R_{VR} = \frac{A_L^2\alpha^2(1-\xi^2)^2}{\sqrt{2}\beta D^2}\exp\left(-\frac{\alpha^2(1-\xi^2)^2}{4\beta D}\right). \tag{8}$$

It is seen that R_{VR} is a nonmonotonic function of ξ as shown experimentally in [13]. Obviously, the expression (8) can be used for an evaluation of R_{VR} for $\xi<1$, since for $\xi\geqslant 1$the bistability disappears. The maximum SNR ($R_{VR}^{\max}$) obeys the scaling law as a function of the input noise strength D_{in},

$$R_{VR}^{\max} = 2\sqrt{2}e^{-1}A_L^2 D_{in}^{-1}. \tag{9}$$

In order to compare the efficiency of VR versus SR for the SNR, we introduce the ratio R_{SNR} defined as

$$R_{SNR} = R_{VR}^{\max}/R_{SR}^{\max}, \tag{10}$$

where $R_{SR}^{\max}$ is the maximum of SNR in SR, $R_{SR}^{\max} = 32\sqrt{2}A_L^2\beta e^{-2}$ follows from (6). Finally,

$$R_{SNR} = (\alpha^2 e/16\beta)D_{in}^{-1}. \tag{11}$$

From the condition $R=1$ it follows that for all $D_{in}^* < \alpha^2 e/16\beta = eV_0/4$, the R_{VR} is always higher than the R_{SR}, since for the R_{SR} the optimal value $D_{SR}^* = V_0/2 < D_{in}^*$.

The experimental setup is essentially the same as was used earlier for the investigation of VR [13]. We studied the laser response after polarization selection when the mixture of two periodic signals with very different frequencies and noise were applied to the injection current. The square-wave and sinusoidal LF signals have a frequency $\Omega_L=1$ kHz and a subthreshold amplitude A_L, whereas the sinusoidal HF control signal has a frequency $\Omega_H=100$ kHz and an amplitude A_H. In what follows, we use the normalized amplitudes of the LF and HF signals defined as $\varepsilon=A_L/\mu_L$ and $\xi=A_H/\mu_H$, where μ_L and μ_H are the switching thresholds at the frequencies Ω_L and Ω_H, respectively, and the noise strength D defined as $D=\sigma_N^2$, where σ_N is the noise amplitude. The normalized amplitude ξ is a control parameter. We tune the injection current of the laser into the middle of the bistability region [15], so that the switching between two polarization states could be induced by the deterministic modulation and noise. The laser responses were detected by a fast photodetector and were recorded further by a digital oscilloscope coupled with a computer to store and process the data. Each point of SNR was obtained by averaging over 10 signals containing 50 000 sampling points with 20 periods of the LF signal. For comparison purposes, we define the SNR for sinusoidal and square-wave signals as $\mathrm{SNR}=I(\Omega_L)/I_N(\Omega_L)$, where $I(\Omega_L)$ and $I_N(\Omega_L)$ are the response of the system to the LF signal and the noise background at the frequency Ω_L, respectively, which were evaluated from the power spectra of the Fourier-transformed time series. The SNR gain due to VR is defined as $G_{SNR}=R_{VR}^{\max}/R_{in}$ (where R_{in} is SNR in the input).

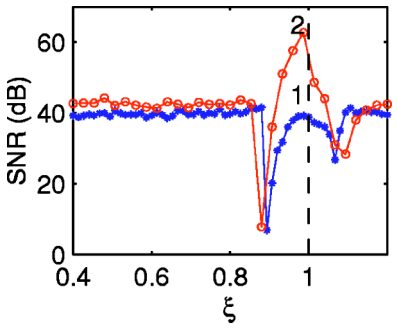

FIG. 1. (Color online) Experiment. SNR for (1) sinusoidal and (2) square-wave LF signals as a function of ξ ($\varepsilon=0.2$). The noise strength $\sigma_N=14$ mV_{rms}. The vertical line marks the transition from bistable (left) and monostable (right) operation.

The experimentally measured SNR due to VR for sinusoidal and square-wave LF signals is shown in Fig. 1. For both types of signals as ξ increases SNR passes through a maximum in the close vicinity of the bifurcation point $\xi=1$ corresponding to the transition from bistability to monostability. For the sinusoidal signal $R_{VR}^{\max}$ is lower than the R_{in}, whereas for the square-wave signal we have a substantial increase of R_{VR}. The second peculiarity is that on both sides from the maximum, R_{VR} practically does not depend on ξ and remains almost constant, which corresponds to the linear response in the bistable and monostable regime.

In Fig. 2, the SNR for the weak square-wave LF signal ($\varepsilon=0.2$) with increasing the level of noise is shown. For a weak noise strength, one can observe a strong increase of SNR with respect to SNR_{in}. This rise takes place exactly where a parametric amplification appears in the bistable system (near the onset of bistability controlled by the HF modulation). A further increase of D (for a moderate level of noise) leads to a degradation of SNR. One can note also the curve broadening and the shift of the optimal value of ξ corresponding to $R_{VR}^{\max}$.

A comparison of the efficiency of VR with respect to SR,

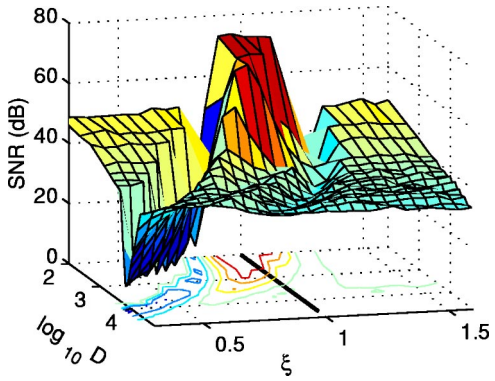

FIG. 2. (Color online) Experiment. The SNR for the square-wave LF signal as a function of ξ and D ($\varepsilon=0.2$). The line in the plane marks the transition from bistability to monostability.

which is characterized by the magnitude R_{SNR} defined by (10), is shown in Fig. 3(a) for both types of the LF signal. It is seen that $R_{SNR}>1$ in the whole range of the input noise strength D. The $R_{VR}^{\max}$ due to VR is always higher than the $R_{SR}^{\max}$, in agreement with the analytical considerations. For weak input noise, R_{SNR} for square-wave signal significantly exceeds the one for the sinusoidal signal, whereas for a moderate noise level R_{SNR} is almost the same for both types of LF signals. The dashed line in Fig. 3(a), (with a slope -1), fits well the experimental data in the range of the moderate noise level, showing agreement with (11) and, correspondingly, with (9) for the noise-induced degradation of SNR.

The experimental evidence of the SNR gain with respect to the SNR_{in} is presented in Fig. 3(b), where G_{SNR} as a function of D for different values of the amplitudes of the square-wave LF signal is shown. For the purpose of comparison, G_{SNR} for the sinusoidal signal is also plotted. First of all, one can note that the relationship $G_{SNR}\gtrsim 1$ is observed for all amplitudes of the LF signal used in the experiment. The unity gain in the SNR is shown by a dashed line in Fig. 3(b). One can stress that for $\varepsilon\approx 0.32$, $G_{SNR}\gg 1$ in the whole range of the noise strength D.

In order to check the validity of our analytical and experimental results we performed a numerical simulation in the framework of Eq. (1),

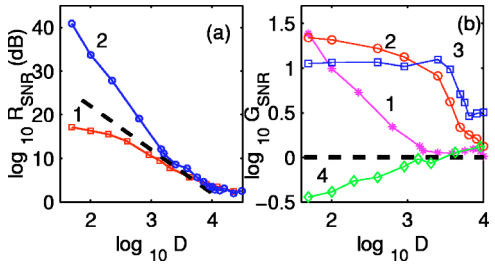

FIG. 3. (Color online) Experiment. (a) R_{SNR} vs D for (1) sinusoidal ($\varepsilon=0.028$) and (2) square-wave ($\varepsilon=0.08$) LF signals. A dashed line is plotted with a slope -1 (see text). (b) G_{SNR} vs D for square-wave
[$\varepsilon=0.08$ (1), 0.2 (2), 0.32 (3)] and sinusoidal [$\varepsilon=0.2$ (4)] LF signals.

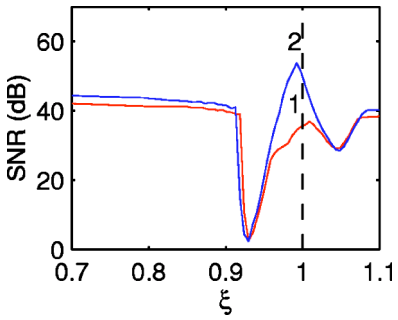

FIG. 4. (Color online) Numerics. SNR vs ξ for the (1) sinusoidal and (2) square-wave LF signals ($D=0.001$, $A_L=0.05$). The vertical line is as in Fig. 1.

$$dx/dt = 4(x - x^3) + A_L F(t) + A_H \sin \Omega_H t + \zeta(t), \qquad (12)$$

where $F(t)=\sin \Omega_L t$ or $F(\Omega_L t)=\mathrm{sgn}(\sin \Omega_L t)$; $\mathrm{sgn}(x)$ is a signum function $\mathrm{sgn}(x)=-1$, for $x<0$, and $\mathrm{sgn}(x)=1$, for $x>0$, $\zeta(t)$ is white, Gaussian noise with $\langle \zeta(t)\zeta(t')\rangle = 2D\delta(t-t')$ and a zero mean $\langle \zeta(t)\rangle = 0$. In what follows, we use the normalized amplitudes ε and ξ defined as $\varepsilon = A_L/\mu_L$ and $\xi = A_H/\mu_H$ where μ_L and μ_H are the switching thresholds at the frequencies $\Omega_L/2\pi=0.001$ and $\Omega_H/2\pi=0.1$, respectively, used in the simulation. A forward Euler algorithm with a fixed step of $0.0012\pi/\Omega_H$ was used. All quantities used for the characterization of the SNR gain in the simulation are defined in the same fashion as before.

A comparison of the SNR due to VR for sinusoidal and square-wave signals is shown in Fig. 4. In accordance with the experimental results depicted in Fig. 1, the SNR for both signals displays the resonancelike behavior depending on ξ. Both maxima are located near the critical value ($\xi=1$) of a switching threshold corresponding to the transition from bistability to a monostable operation. At the same time, in agreement with experimental results, the maximum of SNR for the square-wave signal substantially exceeds the $(\mathrm{SNR})_{in}$, while for the sinusoidal signal the maximum of SNR is lower than the $(\mathrm{SNR})_{in}$. Figure 5 displays the SNR as a function of ξ and D for the square-wave signal with $\varepsilon=0.2$. In qualitative agreement with the experimental results (Fig. 2), there is some range of D, where $(\mathrm{SNR})_{out}\gg(\mathrm{SNR})_{in}$. A strong degra-

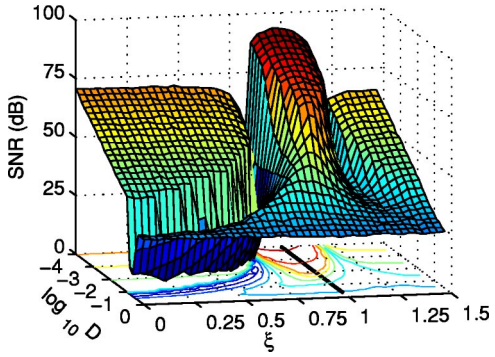

FIG. 5. (Color online) Numerics. SNR_{VR} for the square-wave LF signal as a function of ξ and D ($\varepsilon=0.2$). The line in the plane marks the transition from bistability to monostability.

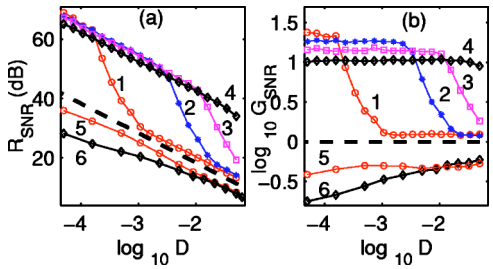

FIG. 6. (Color online) Numerics. (a) R_{SNR} and (b) G_{SNR} for the square-wave
[$\varepsilon=0.032$ (1), 0.125 (2), 0.32 (3), 0.48 (4)] and sinusoidal [$\varepsilon=0.032$ (5), 0.32 (6)] LF signals vs the noise strength D. A dashed line in (a) is plotted using the expression (11).

dation of SNR and the shift of the maximum of SNR to lower values of ξ with increasing D are also observed. In Fig. 6(a) a comparison of the efficiency of VR with respect to SR is shown for different values of the amplitude of square-wave and sinusoidal LF signals. A dashed line in Fig. 6(a) is plotted using the expression (11). It is seen that $R_{SNR} \gg 1$ in the whole range of D and for all values of ε used in the simulation. This means that the $R_{VR}^{\max}$ is always higher the $R_{SR}^{\max}$. One can note also SNR in VR from square-wave signals is always higher than for sinusoidal ones. We can conclude also that an analytical prediction can be considered as a limiting case for weak periodic signals. For square-wave signals it can be considered as the lower bound of R_{SNR}, while for sinusoidal signals as the upper one. In the quasistatical regime of the excitation of VR from the condition $Ax \ll D$ one can find that for $D^* \gg (2/3)^{3/2}(\alpha^2/\beta)\varepsilon^{3/2}$ the expression (11) can be used for the evaluation of R_{SNR}.

The results of the simulation presented in Fig. 6(b) confirm our experimental observation of the SNR gain for square-wave signals. First of all, one can stress that the relationship $G_{SNR} \gtrsim 1$ holds for all amplitudes of the LF signal, even for a very weak signal [$\varepsilon=0.032$, curve 1 in Fig. 6(b)], where the unity gain in the SNR is shown by a horizontal line. On the other hand, going from $\varepsilon \approx 0.3$ to higher values of the amplitude LF signal, G_{SNR} substantially exceeds the unity in the broad range of D, and for $\varepsilon \gtrsim 0.4$ the magnitude G_{SNR} practically does not depend on D. At the same time for sinusoidal signals such an improvement is not observed in the same range of the amplitudes [curves 5 and 6 in Fig. 6(b)].

To conclude, we have shown that the phenomenon of vibrational resonance can represent an effective approach for the detection of weak noisy square-wave signals, allowing to get simultaneously a gain in the SNR and the signal amplitude. Besides, our analysis has shown that SNR due to VR is always higher than the one obtained through the use of the phenomenon of SR. From this point of view, we believe that the results presented in this paper can stimulate further theoretical and experimental works in the field, in particular, to optimize the operation of bistable systems for the detection and regeneration of signals affected by noise, as, e.g., in optical communication systems.

This work has been partially funded by the MIUR project FIRB No. RBNE01CW3M_001.

[1] R. Benzi, A. Sutera, and A. Vulpiani, J. Phys. A **14**, L453 (1981); C. Nicolis and G. Nicolis, Tellus **33**, 225 (1981).
[2] K. Loerincz *et al.*, Phys. Lett. A **224**, 63 (1996).
[3] F. Chapeau-Blondeau, Phys. Lett. A **232**, 41 (1997); Int. J. Bifurcation Chaos Appl. Sci. Eng. **9**, 267 (1999).
[4] Z. Gingl, P. Makra, and R. Vajtai, Fluct. Noise Lett. **1**, L181 (2001).
[5] J. Casado-Pascual *et al.*, Phys. Rev. E **67**, 036109 (2003); Phys. Rev. Lett. **91**, 220601 (2003); Phys. Rev. E **68**, 061104 (2003).
[6] Z. Gingl, R. Vajtai, and L. B. Kiss, Chaos, Solitons Fractals **11**, 1929 (2000).
[7] I. A. Khovanov and P. V. E. McClintock, Phys. Rev. E **67**, 043901 (2003).
[8] P. S. Landa and P. V. E. McClintock, J. Phys. A **33**, L433 (2000).
[9] M. Gittermann, J. Phys. A **34**, L355 (2001).
[10] A. A. Zaikin *et al.*, Phys. Rev. E **66**, 011106 (2002).
[11] E. Ullner *et al.*, Phys. Lett. A **312**, 348 (2003).
[12] J. P. Baltanas *et al.*, Phys. Rev. E **67**, 066119 (2003).
[13] V. N. Chizhevsky, E. Smeu, and G. Giacomelli, Phys. Rev. Lett. **91**, 220602 (2003).
[14] L. Gammaitoni *et al.*, Rev. Mod. Phys. **70**, 223 (1998).
[15] S. Barbay, G. Giacomelli, and F. Marin, Phys. Rev. E **61**, 157 (2000).